VII International Conference on Computational Methods in Marine Engineering
MARINE 2017
M. Visonneau, P. Queutey and D. Le Touzé (Eds)

NUMERICAL ASSESSMENT OF PROPELLER-HULL INTERACTION AND PROPELLER HUB EFFECTS FOR A TWIN SCREW VESSEL

MARINE 2017

HEINRICH STRECKWALL*, YAN XING-KAEDING*, THOMAS LÜCKE*, TOMASZ BUGALSKI†, TOM GOEDICKE‡ AND ALAZ TALAY§

*HSVA, Bramfelder Str. 164, 22305 Hamburg/Germany
e-mail: streckwall@hsva.de

† CTO, Szczecińska 65, 80-392 Gdańsk/Poland
e-mail: tomasz.bugalski@cto.gda.pl

‡ MMG, Teterower Str. 1, 17192 Waren (Müritz)/Germany
e-mail: goedicke@mmg-propeller.de

§ MILPER, Sanayi Mah.Teknopark Blvd. 1, Pendik 34906, Istanbul/Turkey
e-mail: alaz.talay@milper.com.tr

Key words: Relative rotative efficiency, propeller hub, hub vortex, self-propulsion, twin screw.

Abstract. A numerical study that addresses twin screw propulsion was conducted and results using the RANS solvers 'FreSCo+' and 'Fluent' were shared. In order to avoid potential problems on property rights we combined the DTMB (David Taylor Model Basin) model No. 5415 and the SVA (Potsdam Model Basin) propeller No. CPP 1304. The computational self-propulsion point was identified via a numerical implementation of the so-called 'British Method'. In this particular case, linked to the hub dimensions of the chosen propeller, the detailed modelling of the propeller hub and the true resolution of its connection to the hull was rather important. The same view holds for the propeller open water test setup. For the latter case we learned that the comparison with uncorrected experimental thrust data could represent a better way to confirm the numerical results.

1 INTRODUCTION

Experimental and numerical results on the twin screw vessel model DTMB 5415 usually address its manoeuvring performance (see e.g. [1]). Data on pure self-propulsion are rare for DTMB 5415 and the best one can get from literature on thrust and torque at the installed propeller may be found in reference [2]. However we decided to base a common numerical self-propulsion study on DTMB 5415 using the RANS solvers 'FreSCo+' [3] and 'Fluent'. The integration of a suitable twin screw propeller, which not only had to fit to operational requests but also had to satisfy CAD needs on blade surface and hub, was one of our demanding tasks. Viewing the quality of the CAD representation and the unrestricted availability of the CAD data, the SVA (Potsdam Model Basin) propeller CPP1304 was chosen for such a comparative study run in different institutions.

It was agreed to rely on Double Body (DB) setups as the modelling of the rotating propeller introduced already a sufficient amount of complexity. Due to the general lack of propulsion test data, self-propulsion shaft frequencies suitable for CPP 1304 behind DTMB model 5415 were rather to be evaluated than to be prescribed. However we maintained the DB approach and the final scheme to relate a given ship speed to the propeller shaft frequency resembles the 'British Method' known from towing tank tests. Accordingly in our simulation the propulsion point is not directly met but interpolated from DB runs with fixed shaft frequency, representing overload and underload settings. Introducing the 'British Method' to control a numerical process one may save time and resources.

2 PROPELLER OPEN WATER TEST AND RESULTS FROM CFD SIMULATION

The findings from this section suggest a certain caution when comparing RANS simulations on open water (OW) tests and related experiments. Similar to the RANS treatment of propulsion tests discussed further below we set emphasis on the propeller hub details entering the numerical grids. For the evaluation of the numerically treated OW-mode one should request 'uncorrected' thrust data from the OW tests. Such uncorrected data where available for CPP 1304 and finally entered the comparison of measured and calculated OW curves.

2.1 Propeller 1304 as an example for hub effects in Open Water mode

The larger the boss dimensions of the propeller the higher the risk to invoke errors when doing manipulations in the hub area for convenience. This caution was already stressed by the authors in a contribution to NuTTS'16 [4]. Geometrical as well as experimental data for the CPP 1304 of the Potsdam Model Basin (SVA) were available from the Potsdam website. This propeller served for several benchmarks on OW computation, cavitation analysis and (latest) propeller-scaling (see for instance [5]). The geometry was documented including all details on shafting, nose cap and on the gap between rotating and fixed parts of the OW-setup.

Table 1: Particulars propeller 1304 ('Model Scale OW' existing as hardware; other scales are hypothetic)

	FS (behind)	**FS (OW)**	**Model Scale (behind)**	**Model Scale (OW)**
Type	CP	CP	CP	**CP**
No. of blades	5	5	5	**5**
D (m)	5.10	3	0.2055	**0.25**
P/D (0.7R)	**1.635**	**1.635**	**1.635**	**1.635**
Ae/A0	0.779	0.779	0.779	**0.779**
Rotation	inw/outw	right	inw/outw	**right**
Hub ratio	0.3	0.3	0.3	**0.3**

Table 1 gives the main particulars of CPP 1304. Only the column titled ‘Model Scale OW’ relates to an existing hardware. The other scales are hypothetic as the table also reflects dimensions related to full scale OW calculations and to a ‘fitted’ version of CPP 1304 (smaller diameter) which is entering in-behind studies (together with the DTMB 5415 appended hull). As a comparison of the CPP 1304 performance in OW and in-behind was planned from the start, the OW case was treated in two alternative ways, namely using a single domain rotating on the whole and two domains (one rotating cylindrical volume around propeller and hub and one large fixed volume) connected by sliding interfaces. In any case the grids around the blades were adjusted to resolve the laminar sub-layer in model scale, i.e. the cells at the wall show $y^+ \approx 1$.

K_T and K_Q from the experiment were available with and w/o hub correction. As usual K_T represents a normalized thrust defined as

$$K_T = T/(\rho n^2 D^4) \quad (1)$$

The torque coefficient K_Q normalises the Torque similarly

$$K_Q = Q/(\rho n^2 D^5) \quad (2)$$

As the OW tables delivered from EFD usually isolate the blade forces we separated the blades also in the post processing of the CFD output. The K_T -comparison of EFD and CFD on this basis is given in Figure 1 by the dashed lines. For the CPP 1304 also uncorrected measurements were available, which logically included blade and hub forces as a total. Adding the hub parts in the CFD post processing and doing the ‘Blades&Hub’-comparison gives the full lines in Figure 1, which reflect a much better agreement. The reason, why a hub correction performed in EFD - on the basis of an isolated hub run - may isolate the blade forces insufficiently is demonstrated with Figure 2. It gives a sample for a typical pressure field developing on the nose cap and entering the total thrust balance. In this view the blades have been removed to isolate the cap surface, but they actually trigger the pressure on large parts of the cap. The moments are hardly effected by geometrical details for the hub and a good agreement on K_Q was already obtained on the basis of the ‘corrected’ EFD data.

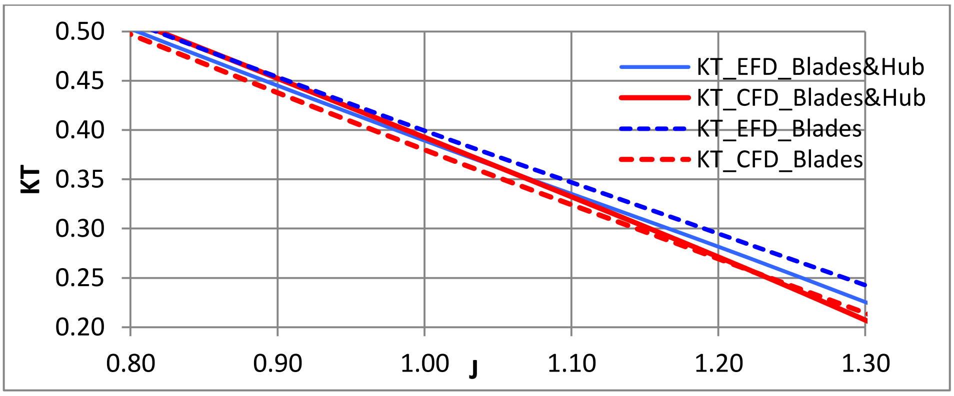

Figure 1: Thrust coefficient KT in EFD and CFD (FresCo+-results) for model scale, referencing on one hand only forces on blases (‘Blades’) and on the other hand blades and hub forces (‘Blades&Hub’).

2.2 Propeller 1304 in hypothetic Open Water modes

It was planned to run a hypothetic model scale self-propulsion simulation where the propeller shows a ‘slip wall’ boundary condition while hull and appendages are treated ‘non-slip’ as usual. To process the related in-behind propeller performance data a similar hypothetic OW scenario was required. Figure 3 shows open water results calculated for model scale under ‘non-slip wall’ and ‘slip wall’ settings. Besides K_T and K_Q also the OW efficiency η_o is given ($\eta_o = (T\,u)/(2\pi n Q)$, u denoting the advance velocity). Figure 3 includes a true full scale case using dimension D=3 m and shaft frequency n=4.33 1/s. These settings reflect the demands of a recent ITTC benchmark call on propeller scaling (based on CPP 1304).

According to Figure 3 we obtained nominally higher scale effects on thrust (thrust coefficient K_T) than on torque (torque coefficient K_Q) while the full-scale efficiency was behaving as expected. The ‘slip wall’ case represents a performance extreme, which roughly doubles the efficiency offset already existing between model and full scale, the latter case treated as hydraulically smooth here.

We also dealt with the hypothetic scenario of a reversed open water setup, which resembles the combination of blades, hub and cap from the propulsion mode (Figure 4). For the isolated blade forces and moments we found hardly any difference in this case.

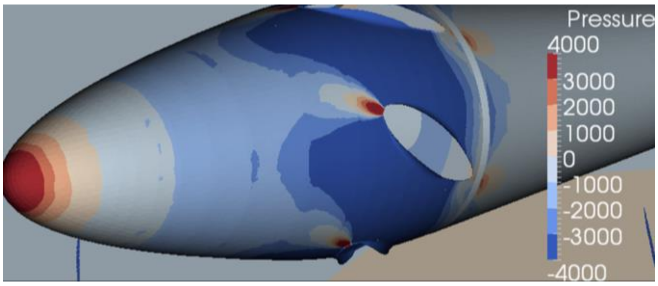

Figure 2: Pressure on nose cap of CPP 1304 in POW mode (flow from left to right)

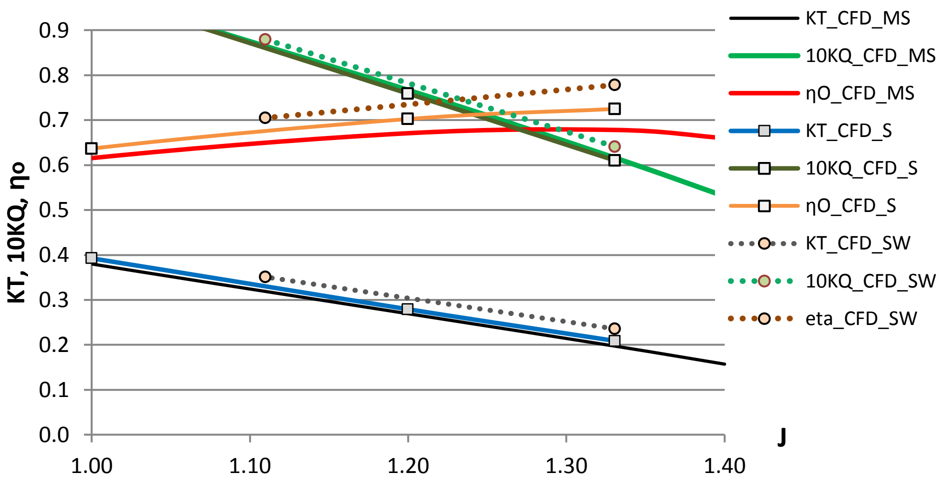

Figure 3: Open Water calculations in different scale: ‘MS’ for Model Scale, ‘S’ for full scale and ‘SW’ for a slip wall condition set on the blade surface (FreSCo+-results)

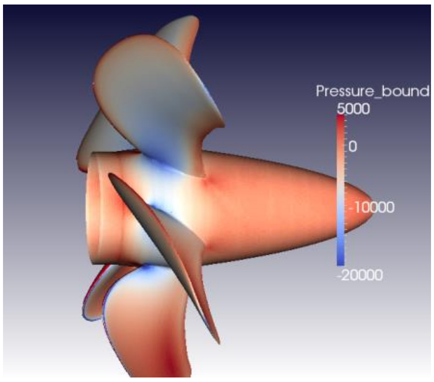

Figure 4: Setup for Open Water calculations in 'reversed mode'

3 PROPELLER 1304 BEHIND HULL DTMB 5415

In order to compare results of different institutions the in-behind setup was prescribed in terms of model speeds, geometry of hull and appendages, propeller position as well as propeller blade- and hub-details. Grids were generated under the demand, that the laminar sub-layer on the propeller blade surface should be resolved ($y^+ \approx 1$). However the connection of the rotating propeller to the cylindrical strut barrel and the shaft was meshed differently. For the setup treated with Fluent a complete gap upstream of the propeller close to the blade root sections was introduced. For the scenario treated with FreSCo$^+$ initially, a gapless connection was set at that point. The Fluent results on thrust showed a strong response to this mesh detail and so did the so-called 'small figures', in particular the 'relative rotative efficiency' η_R and the wake fraction. We recall that η_R represents the ratio of OW and in-behind torque coefficients at K_T-Identity:

$$\eta_R = K_Q^{OW}/K_Q^{BH} \tag{3}$$

To be comparable with the setup used for Fluent, the FreSCo$^+$ analysis was recently also done with gap as well. In this analysis a centre shaft was added, closing the gap near the axis.

3.1 Numerical treatment of self-propulsion

Self-propulsion of the DTMB 5415 vessel was considered in model scale. Table 2 gives the main particulars for the hull in model and full scale. As already listed in Table 1 the combination of DTMB 5415 and propeller CPP 1304 was established under the assumption that the full scale diameter should read D_{FS} =5.1 m.

In view of a numerical 'British Method' serving to find the self-propulsion point, two suitable shaft frequencies were to be estimated for every ship speed. To meet the actual self-propulsion point by linear interpolation, the lower estimate should represent a state with insufficient propeller thrust and the higher guess should resemble a state with too highly loaded propeller. Using the OW data of CPP 1304 and referencing results on thrust coefficient

K_T and shaft frequency *n* related to full scale propulsion of DTMB 5415 with another propeller [2] we arrived at the shaft frequency guesses given in Table 3. As model scale propulsion was simulated under the DB approach this table also includes offset forces. To define self-propulsion they are to be added to (resp. subtracted from) the numerical derived hull forces. These offsets consist of a friction deduction force F_D derived by HSVA and an estimate of the pure wave resistance of the hull derived by two phase flow calculations on hull resistance using Fluent. According to Table 3 the self-propulsion point is related to a positive offset $F_{HULL} - T_{TOTAL}$ for Froude number Fn=0.28 and to a negative offset $F_{HULL} - T_{TOTAL}$ at Fn=0.41 (T_{TOTAL} stands for the thrust of the twin screw system).

The grids generated for Fluent and FreSCo+ consisted of two domains connected by sliding interfaces, namely a rotating cylinder for the cells around propeller and hub and a fixed cell system for the remaining flow regime. We applied two alternatives for the effective treatment of the rotating propeller while the hull flow develops. The 'frozen rotor' and the rotor driven by a 'ramp'-function (reducing initially large time steps continuously) were the applied techniques to reduce the computational time.

Table 2: Particulars of DTMB 5415 in Full Scale and Model Scale (λ=24.825)

	FS	**MS**
Lpp (m)	142	5.719
Lwl (m)	142.18	5.726
Bwl (m)	19.06	0.768
T (m)	6.15	0.248
S w/o rudder (m^2)	2972.6	4.823

Table 3: Conditions for Model Scale propulsion (Fn, V, n), estimated performance of (one) propeller (w_e. K_T, T_1) and DB propulsion point in terms of F_{HULL}-T_{TOTAL} (involving wave resistance R_r and friction deduction FD)

Fn[ ]	V [m/s]	n[1/s]	We (estimate)	J	T_1 in OW [N]	KT	FD[N]	Rr [N] (estimate)	F_{HULL}-T_{TOTAL} =FD-Rr [N]
0.28	2.094	7.288	0.04	1.342	19.3239	0.204	11.85	8.50	3.38
0.28	2.094	7.943	0.04	1.232	29.9294	0.266	11.85	8.50	3.38
0.41	3.071	11.724	0.04	1.224	66.1855	0.27	22.72	80.00	-57.42
0.41	3.071	12.88	0.04	1.114	97.3363	0.329	22.72	80.00	-57.42

3.2 Results on numerical self-propulsion

A first interesting finding from the common test case treatment is given by the history of the single blade forces as displayed in Figure 5 (showing higher fluctuations than expected). It was also interesting to check propeller forces in detail and investigate gap effects. The treatment of the gap between the hub and the strut barrel (modelled or not) will not influence the self-propulsion point (in view of the resulting shaft frequency) but it will affect the thrust dedicated to the propeller unit. All Fluent results on self-propulsion at the speeds and shaft frequencies covered by Table 3 were obtained with a complete gap between propeller hub and shaft barrel (see Figure 6). The mid picture of this figure already indicates the negative pressure acting on the gap disc representing part of the propeller hub. When the self-propulsion point was deduced from the DB Fluent-calculations at Fn=0.28 and Fn=0.41 we used the forces offsets $F_{HULL} - T_{TOTAL}$ given in Table 3. According to Figure 7 representing outward turning propellers at Fn=0.41 the 'British Method equivalent' self-propulsion point was obtained at T_1=93.04 N. Note, that in this figure only half of the offset force is plotted on the horizontal axis as only one propeller is referenced.

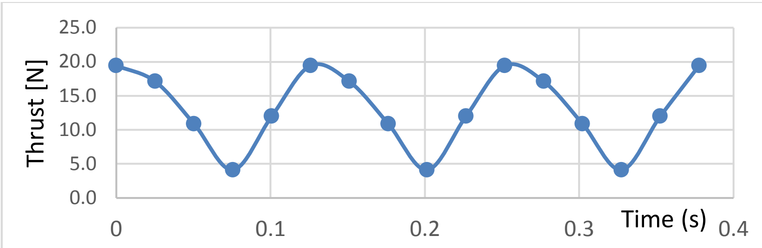

Figure 5: DB Fluent-calculations for outward turning at n=11.72 [1/s]**:** generating an equivalent single blade thrust history by analysing individual blade thrusts at one time step

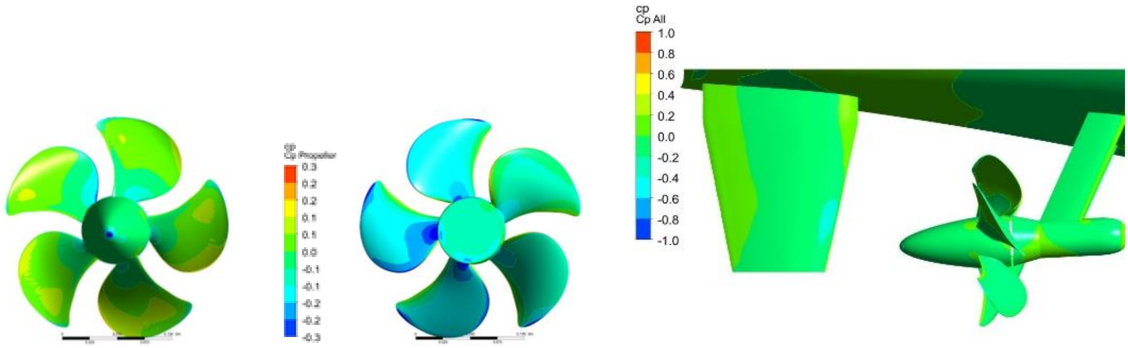

Figure 6: DB Fluent-calculations addressing gap effects at outward turning twin-screw propeller at Fn=0.41: pressure on hull/propeller without gap (left) and with gap (right)

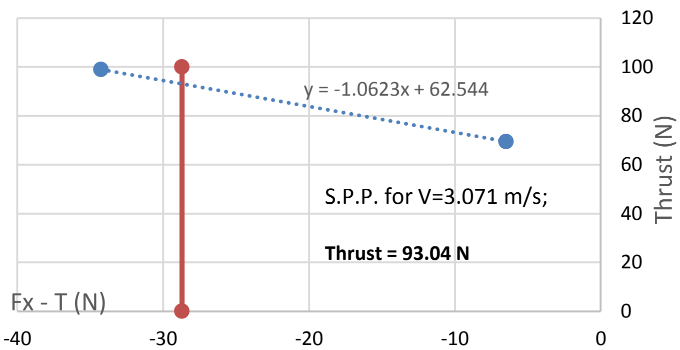

Figure 7: DB Fluent-calculations for outward turning at Fn=0.41: evaluation of propeller thrust at self-propulsion via linear interpolation in a 'thrust over (hull force minus thrust)'-diagram following the 'British method' known from towing tank experiments.

The FreSCo$^+$-calculations did not include the gap initially. The analysis with FreSCo$^+$ was then repeated on a grid which shoes a 3 mm gap in model scale (HSVA's standard for propulsion test setups). To comply with test setups, the gap was closed by a shaft dummy in the vicinity of the shaft axis. According to Figure 8 the DB FresCo$^+$-calculations hardly show any global difference in the pressure on hull, shaft and rudder when comparing without gap (left picture) and with gap (right picture). The detailed visualization done in Figure 9 confirms, that the pressure in the gap ranges on a quite constant and negative level, as already recognized for the Fluent results. In return, a corresponding low pressure has also been detected for the opposite gap disc belonging to the ship. Consequently the force balance for the whole system does not change with or without gap, neither does the self-propulsion point.

3.3 Further processing of data from numerical self-propulsion

Depending on the shaft frequency setting, we noticed an increase of the propeller thrust by about 3-7% when the force on the gap is added. By including the gap and following the model test evaluation procedure, we typically identify an increase in 'relative rotative efficiency' η_R by about 4 %. Figure 10 gives an example on the η_R-results for an outward turning case at Fn=0.41 and n_2=12.10 1/s (interpolated self-propulsion point from FreSCo$^+$-results). According to this figure the lowest η_R-value is obtained when neglecting of the gap force and including the forces on the downstream cap. The η_R-value from 'blades only' ranges slightly higher than the latter. Note, that in any case the 'blades only' K_T and K_Q were referenced in the computed model scale OW results.

As announced above an in-behind analysis was done using FreSCo$^+$ giving the propeller blades a 'slip wall' boundary condition. For the outward turning case at Fn=0.41 the Figure 11 shows η_R-results obtained at the two shaft frequencies either combining 'slip wall' propulsion with 'slip wall' OW or 'regular' propulsion with 'regular' OW. The artificial 'slip wall' setting does not change the η_R-results too much (the isolated dependence on the shaft frequency shows similar differences).

4 CONCLUSIONS

Summarizing one may state that more strictly than initially expected the system of blades and hub must be taken as a unit and geometrical details around the hub must be carefully reflected to allow for a true comparison of EFD and CFD. For model scale propulsion as well as for OW the grids around the blades were adjusted to resolve the laminar sub-layer. This high resolution request is connected to superior efforts in grid generation and to probably enlarged computation time. Depending on the concerns – above we put some stress on η_R - the 'slip wall' setting may represent a chance to ease the numerical propulsion simulations.

ACKNOWLEDGEMENTS

This work is linked to the INRETRO project realized as a European ERA-NET venture in the MARTEC framework. The financial support by the national funding associations is gratefully acknowledged.

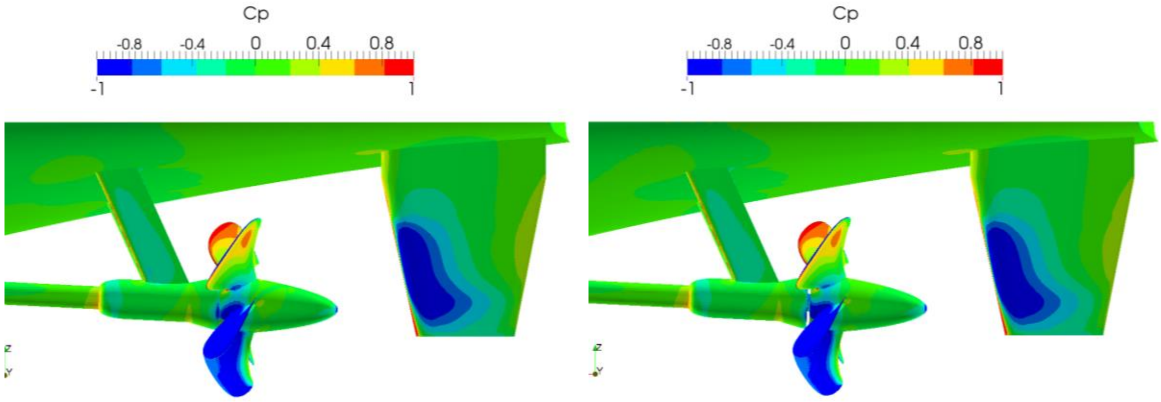

Figure 8: DB FresCo^{+}-calculations addressing gap effects at outward turning twin-screw propeller at Fn=0.41: pressure on hull/propeller without gap (left) and with gap (right)

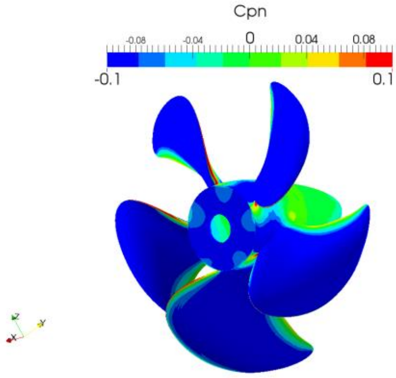

Figure 9: FresCo^{+}-calculations with resolved gap for propeller in propulsion mode indicating negative pressure in the gap.

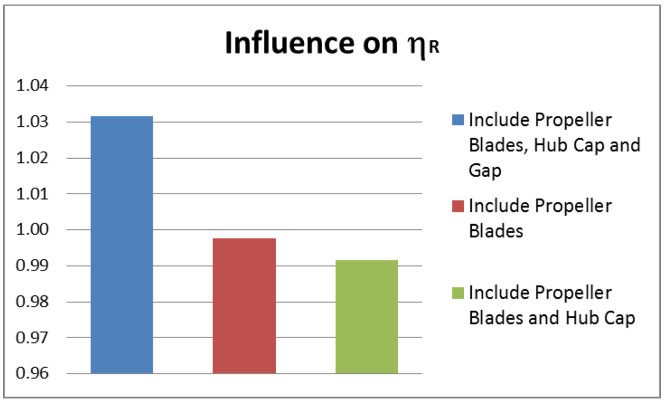

Figure 10: DB FreSCo^{+}-calculations in model scale, outward turning with n=12.10 1/s (interpolated self-propulsion point at Fn=0.41): evaluation of η_R with and without reference to hub-parts (in the latter case either 'Hub Cap & Gap' or 'Hub Cap only')

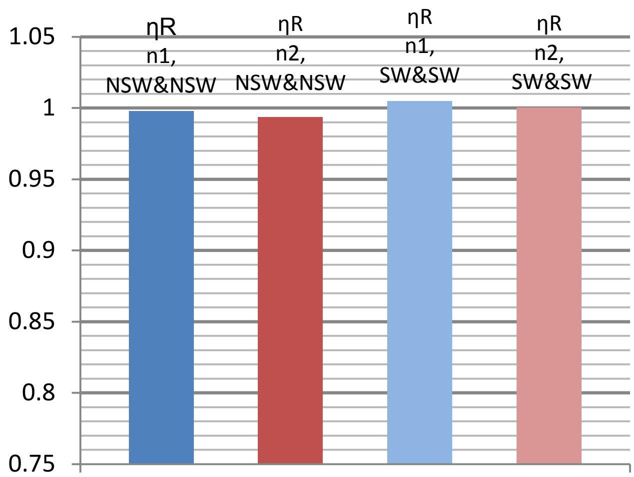

Figure 11: DB FreSCo+-calculations in model scale for outward turning with n_1=11.72 [1/s] resp. with n_2=12.88 [1/s] (Fn=0.41): evaluation of η_R *without* reference to hub-parts using either the combination 'non-slip wall OW'&'non-slip wall behind' or 'slip wall OW' & 'slip wall behind'

REFERENCES

[1] Benedetti, L., Bouscasse, B., Broglia, R., Fabbri, L., La Gala, F., and Lugni, C., *PMM Model Test with DDG51 Including Uncertainty Assessment*, INSEAN Technical Report, (2007).

[2] Gheriani, E., *Fuel Consumption Prediction Methodology for Early Stages of Naval Ship Design,* Massachusetts Inst. of Techn. (MIT), Master of Science Thesis, (2012).

[3] Hafermann, D., *The New RANSE Code FreSCo for Ship Application*, STG Jahrbuch (2007)

[4] Streckwall, H. at al, *Numerical Studies on Propellers in Open Water and behind Hulls aiming to support the Evaluation of Propulsion Tests*, 19th Numerical Towing Tank Symposium NuTTS'16, Oct. 3-4, St. Pierre D'Oleron, France (2016)

[5] Maksoud, M., *Proceedings of the Workshop on Cavitation and Propeller Performance*, 2nd International Symposium on Marine Propulsors - smp'11, Hamburg, Germany (2011)